Incorporation of Non-Steady-State Unimolecular and Chemically Activated Kinetics into Complex Kinetic Schemes. 1. Isothermal Kinetics at Constant Pressure

Vadim D. Knyazev*

The Catholic University of America, Department of Chemistry, Washington, DC 20064

Wing Tsang

National Institute of Standards and Technology, Physical and Chemical Properties Division, Gaithersburg, Maryland 20899

Received: November 13, 1998; In Final Form: March 12, 1999

A general method of accounting for non-steady-state unimolecular kinetics of reactive species in complex kinetic schemes is described. The method is based on dividing the overall population of affected species into virtual components corresponding to individual eigenvectors of the master equation matrix. It is shown that these individual virtual components are in their respective steady states and evolve independently of each other. The overall treatment is significantly simplified by the fact that only several of these virtual components need to be considered explicitly, and the contribution of the remainder can be described jointly as resulting in ordinary chemical branching. The described method reduces the problem of non-steady-state kinetics to a modest kinetic scheme which can be solved by standard techniques.

I. Introduction

At sufficiently high temperatures or low pressures, unimolecular and chemically activated reactions are characterized by non-steady-state behavior[1−6] when the characteristic time of reaction becomes comparable with or shorter than the time required for the population energy distribution to achieve its steady state. This results in the inapplicability of traditional methods of describing the kinetics of these reactions since the very notion of time-independent rate constants becomes invalid. Instead, the kinetics of such elementary reactions becomes characterized by a complex concentration vs time dependence controlled by an interplay of formation, decay, and collisional relaxation/excitation processes which need to be accounted for at an energy-resolved level. Moreover, the kinetic fate of the same species formed in different reactions can be different due to different energy distributions.[5,6]

Conditions (temperature and pressure) of the onset of non-steady-state effects depend on the particular reactive system being considered. Generally, onset temperatures are lower for reactions with low energy barriers[2,5] and, for several types of reactions, deviations from steady-state behavior can become significant under relatively mild conditions. Kiefer et al.[3] experimentally determined reaction incubation times (non-steady-state effect) in the decomposition of norbornene at temperatures as low as 869 K. Another example of such reactions is the thermal decomposition of hydrocarbon radicals. The rate of *n*-hexyl radical decomposition already deviates from its steady-state value at the temperature 1300 K at 1.01×10^5 Pa[5] (1 atm) and at even lower temperatures if lower pressures are considered. Similarly mild conditions of onset of non-steady-state effects can be expected for chemically activated reactions involving alkyl and substituted alkyl peroxy intermediates (such as $R + O_2 \rightleftharpoons RO_2 \rightarrow$ products) due to the low barriers for RO_2 decomposition.[7]

These effects, therefore, have important consequences for kinetic modeling of complex chemical processes such as combustion. However, at present, no methods are available for quantitatively describing kinetics of complex systems in the presence of non-steady-state effects. In principle, such effects can be accounted for by dividing the energy scale of the molecule of interest into small bins and treating each energy bin as a separate chemical species. Solving the overall kinetics will thus require accounting for all energy-dependent reactions of these pseudospecies, as well as conversions between them due to collisional relaxation/excitation. Such an approach, however, is impractical since the size of the overall kinetic problem becomes prohibitively large due to the necessarily small size of an individual energy bin (which must be smaller than the value of $\langle \Delta E \rangle_{\text{down}}$, an average energy transferred per downward collision with the bath gas).

In the current work, we describe a general method of accounting for non-steady-state kinetics of reactive species in the modeling of complex kinetic schemes. The method is based on dividing the overall population of affected species into virtual components corresponding to individual eigenvectors of the master equation matrix. It is shown that these individual virtual components (1) are in their respective steady states and (2) evolve independently of each other. The overall treatment is significantly simplified by the fact that only several of these virtual components need to be considered explicitly and the contribution of the remainder can be described jointly as resulting in ordinary chemical branching.

The described method reduces the problem of non-steady-state kinetics to a modest kinetic scheme which can be solved by standard techniques. Currently, this method is capable of treating isothermal kinetics at constant pressure. In section II, a general description of the method is presented. Section III describes application of the method to the unimolecular decomposition of *n*-butyl radical (a comparison with the exact

* Corresponding author. E-mail: knyazev@cua.edu.

10.1021/jp984423n CCC: $18.00
Published on Web 04/29/1999

solution of the time-dependent master equation is given) and to the kinetic modeling of the oxidative pyrolysis of an n-C_4H_9I/n-C_4H_{10}/O_2 mixture. Discussion is provided in section IV.

II. Method

The current description of non-steady-state unimolecular kinetics as part of a large kinetic scheme is based on a one-dimensional (in energy only, effects of angular momentum conservation are neglected) master equation describing the interplay of formation, collisional relaxation/excitation, and reaction of active molecules. In many respects, the approach of the current work is based on that of Schranz and Nordholm[1] and Smith et al.[8] In this section, first, a general solution of a time-dependent master equation is described as kinetics of "virtual components" of the overall concentration of active molecules. It is shown that these "virtual components" (related to the eigenvectors of the master equation matrix) are in their corresponding steady states and evolve independently of each other. As a result, the problem of non-steady-state kinetics is reduced to a large kinetic scheme. Then, it is shown that this large kinetic scheme can be substantially reduced in size (to only few reactions) without any loss of accuracy. The resultant smaller kinetic scheme can be included directly in the complex kinetic mechanism of the overall process of interest and solved using standard methods. Finally, a short summary of the algorithm is presented.

II.1. Representation of Non-Steady-State Kinetics by a Large Modified Kinetic Scheme. *II.1.1. Kinetics of the Population Energy Distribution Function.* We consider a complex kinetic model described by a large number of elementary reactions:

$$\begin{cases} \text{Reactants(1)} \xrightarrow{k^1} \text{Products(1)} \\ \cdots\cdots \longrightarrow \cdots\cdots \\ \text{Reactants(m)} \xrightarrow{k^m} \text{Products(m)} \\ \cdots\cdots \longrightarrow \cdots\cdots \end{cases} \quad (1)$$

Let us select those parts of the overall eq 1 (subsets M1, M2, and M3) which describe the evolution of species A characterized by non-steady-state behavior:

$$\begin{cases} \text{Reactants(m1)} \xrightarrow{k^{m1}} A & m1 \in M1 \\ \cdots\cdots \quad \cdots\cdots \quad \cdots\cdots \\ A \xrightarrow{k^{m2}(E)} \text{Products(m2)} & m2 \in M2 \\ \cdots\cdots \quad \cdots\cdots \quad \cdots\cdots \\ A + \text{Reactants(m3)} \xrightarrow{k^{m3}} \text{Products(m3)} & m3 \in M3 \\ \cdots\cdots \quad \cdots\cdots \quad \cdots\cdots \end{cases} \quad (2)$$

Here, A is formed in (possibly, several) reactions indexed by m1 and decays via reactions indexed by m2 and m3 either unimolecularly (m2) or in reactions with other species (m3). In the absence of knowledge of exactly how the energy distribution of A might affect the rates of reactions m3, we will assume that these reactions can be described by simple rate constants k^{m3}.

The master equation describing the interplay between energy-dependent reactions and collisional relaxation/excitation can be written for species A as

$$\frac{\partial g(E,t)}{\partial t} = \int_0^\infty [R(E,E')\, g(E',t) - R(E',E)\, g(E,t)]\, \mathrm{d}E' - k(E)\, g(E,t) + u(t)\, g(E,t) + r(E,t) \quad (3)$$

where $g(E,t)$ is the population of energy level E at time t, $R(E,E')$ is the rate coefficient of collisional energy transfer from energy level E' to energy level E, $k(E)$ is the energy-dependent microscopic rate constant of decay via all reactions m2, $-u(t)$ is the pseudo-first-order rate coefficient of A decay via all reactions m3, and $r(E,t)$ is the energy- and time-dependent rate of formation of A species with a particular energy E.

Equation 3 can be presented in matrix form (here the energy scale is divided into an array of discrete states E_i, each with width δE, and energy-dependent functions are represented by vectors).

$$\frac{\mathrm{d}\mathbf{g}(t)}{\mathrm{d}t} = \mathbf{J}\mathbf{g}(t) + u(t)\mathbf{g}(t) + \mathbf{r}(t) \quad (4)$$

Here, $\mathbf{J}$ is the matrix of a simpler master equation (see ref 9) corresponding to the thermal unimolecular reaction, different channels of which are referenced by indices m2 in eq 2.

$$J_{i,l} = \begin{cases} R(E_i,E_l)\delta E, & i \neq l \\ -k(E) - \delta E \sum_{l \neq i} R(E_l, E_i), & i = l \end{cases} \quad (5)$$

We can note that

$$k(E) = \sum_{\mathrm{m2}} k^{\mathrm{m2}}(E) \quad \text{or} \quad \mathbf{k} = \sum_{\mathrm{m2}} \mathbf{k}^{\mathrm{m2}} \quad (6)$$

$$u(t) = -\sum_{\mathrm{m3}} k^{\mathrm{m3}}[\text{reactants(m3)}] \quad (7)$$

$$\mathbf{r}(t) = \sum_{\mathrm{m1}} k^{\mathrm{m1}}[\text{reactants(m1)}]\mathbf{x}^{\mathrm{m1}} \quad (8)$$

where $\mathbf{x}^{\mathrm{m1}}$ is the energy distribution of A molecules formed in reaction m1 (normalized such that $\delta E \sum_i x^{\mathrm{m1}}(E_i) = 1$). [reactants-(m1)] and [reactants(m3)] are concentrations or products of concentrations of all reactants (other than A) of reactions m1 and m3, respectively. Equation 8 can accommodate various types of excitation mechanisms such as chemical activation (see ref 10 for the functional form of $x^{\mathrm{m1}}(E)$ dependence), thermal activation ($\mathbf{x}^{\mathrm{m1}}$ is given by the Boltzmann distribution), laser excitation ($x^{\mathrm{m1}}(E)$ is a δ-function and [reactants(m1)] becomes a time-dependent laser intensity), etc.

Equation 4 can be transformed into

$$\frac{\mathrm{d}\mathbf{q}(t)}{\mathrm{d}t} = \mathbf{B}\mathbf{q}(t) + u(t)\mathbf{q}(t) + \mathbf{p}(t) \quad (9)$$

via multiplying by $\mathbf{S}$, a diagonal matrix with elements

$$S_{ii} = f_i^{-1/2} \equiv f^{-1/2}(E_i) \quad (10)$$

Here, $\mathbf{f}$ is the normalized ($\delta E \sum_i f(E_i) = 1$) Boltzmann distribution vector, $\mathbf{q}(t) = \mathbf{S}\mathbf{g}(t)$, and $\mathbf{p}(t) = \mathbf{S}\mathbf{r}(t)$. The matrix $\mathbf{B} = \mathbf{S}\mathbf{J}\mathbf{S}^{-1}$ is Hermitian, all its eigenvalues are real and negative, and the corresponding eigenvectors $\mathbf{c}_j$ form a complete orthogonal set (see ref 9 for properties of $\mathbf{B}$ and $\mathbf{J}$) which we choose to be orthonormal ($(\mathbf{c}_{j1},\mathbf{c}_{j2}) = 0$ for j1 $\neq$ j2 and $(\mathbf{c}_j,\mathbf{c}_j) = 1$). (We use here the definition of a scalar product of vectors[11] $(\mathbf{x},\mathbf{y}) = \int_0^\infty x(E)y(E)\,\mathrm{d}E = \sum_i x(E_i)y(E_i)\delta E$) Eigenvalues λ_j of $\mathbf{J}$ coincide with those of $\mathbf{B}$ and eigenvectors of $\mathbf{J}$, $\mathbf{e}_j$, are related to $\mathbf{c}_j$ via $\mathbf{e}_j = \mathbf{S}^{-1}\,\mathbf{c}_j$.

The solution of eq 9 is given (see ref 12, p 380, 384) by

$$\mathbf{q}(t) = \exp[\mathbf{B}t + v(t)\mathbf{I}]\mathbf{q}_o + \int_0^t \exp[\mathbf{B}(t-s) + (v(t) - v(s))\mathbf{I}]\mathbf{p}(s)\,ds \quad (11)$$

where $v(t) = \int_0^t u(s)\,ds$, $\mathbf{q}_o = \mathbf{S}\mathbf{g}_o$, $\mathbf{g}_o$ is the initial population vector, and $\mathbf{I}$ is the unit matrix.

We now expand $\mathbf{p}(t)$ and $\mathbf{q}_o(t)$ in terms of $\mathbf{c}_j$, the eigenvectors of $\mathbf{B}$:

$$\mathbf{p}(t) = \sum_j \theta_j(t)\mathbf{c}_j, \quad \text{where } \theta_j(t) = (\mathbf{p}(t),\mathbf{c}_j) = \sum_i p(E_i,t)c_j(E_i)\delta E \quad (12)$$

$$\mathbf{q}_o = \sum_j \xi_j \mathbf{c}_j, \quad \text{where } \xi_j = (\mathbf{q}_o,\mathbf{c}_j) = \sum_i q_o(E_i)c_j(E_i)\delta E \quad (13)$$

Using the eigenvalue relation $\mathbf{B}\mathbf{c}_j = \lambda_j\mathbf{c}_j$, we obtain from (11)

$$\mathbf{q}(t) = \sum_j \xi_j \exp[\lambda_j t + v(t)]\mathbf{c}_j + \int_0^t \sum_j \exp[\lambda_j(t-s) + v(t) - v(s)]\theta_j(s)\mathbf{c}_j\,ds \quad (14)$$

Multiplying both sides by $\mathbf{S}^{-1}$, we obtain for the population distribution of species A

$$\mathbf{g}(t) = \sum_j \xi_j \exp[\lambda_j t + v(t)]\mathbf{e}_j + \int_0^t \sum_j \exp[\lambda_j(t-s) + v(t) - v(s)]\theta_j(s)\mathbf{e}_j\,ds = \sum_j \mathbf{g}_j(t) \quad (15)$$

where

$$\mathbf{g}_j(t) = \mathbf{e}_j\{\xi_j \exp[\lambda_j t + v(t)] + \int_0^t \exp[\lambda_j(t-s) + v(t) - v(s)]\theta_j(s)\,ds\} \quad (16)$$

The overall population of A molecules is given by summing $g(E_i)$ over all energies:

$$G(t) = \sum_i g(E_i,t)\delta E = \sum_j \Phi_j\{\xi_j \exp[\lambda_j t + v(t)] + \int_0^t \theta_j(s) \exp[\lambda_j(t-s) + v(t) - v(s)]\,ds\} = \sum_j G_j(t) \quad (17)$$

where Φ_j are the sums of all components of the individual eigenvectors $\mathbf{e}_j$

$$\Phi_j = \sum_i e_j(E_i)\delta E \quad (18)$$

and

$$G_j(t) = \Phi_j\{\xi_j \exp[\lambda_j t + v(t)] + \int_0^t \theta_j(s) \exp[\lambda_j(t-s) + v(t) - v(s)]\,ds\} = \sum_i g_j(E_i,t)\delta E \quad (19)$$

Vectors $\mathbf{g}_j(t)$ (and functions $G_j(t)$) can be understood as components of the overall $\mathbf{g}(t)$ population distribution function (and the overall population $G(t)$) corresponding to individual eigenvectors. The temporal evolution of these components can be analyzed by evaluating derivatives of expressions 16 and 19.

$$\frac{d\mathbf{g}_j(t)}{dt} = \mathbf{e}_j\{\xi_j(\lambda_j + u(t)) \exp[\lambda_j t + v(t)] + (\lambda_j t + u(t)) \int_0^t \exp[\lambda_j(t-s) + v(t) - v(s)]\theta_j(s)\,ds + \theta_j(t)\} \quad (20)$$

$$\frac{dG_j(t)}{dt} = \Phi_j\{\xi_j(\lambda_j + u(t)) \exp[\lambda_j t + v(t)] + (\lambda_j t + u(t)) \exp[\lambda_j t + v(t)]\int_0^t \theta_j(s) \exp[-\lambda_j s - v(s)]\,ds + \theta_j(t)\}$$

Comparing these equations with 16 and 19 and noting that $\mathbf{g}_j(0) = \xi_j\,\mathbf{e}_j$ and $G_j(0) = \xi_j\,\Phi_j$, we obtain

$$\frac{d\mathbf{g}_j(t)}{dt} = (\lambda_j + u(t))\mathbf{g}_j(t) + \theta_j(t)\mathbf{e}_j; \quad \mathbf{g}_j(0) = \xi_j\mathbf{e}_j \quad (21)$$

$$\frac{dG_j(t)}{dt} = (\lambda_j + u(t))G_j(t) + \theta_j(t)\Phi_j; \quad G_j(0) = \xi_j\Phi_j \quad (22)$$

As can be seen from eqs 15−19 and 21−22, the population $G(t)$ of species A can be considered as composed of components corresponding to the individual eigenvalues λ_j of the matrix $\mathbf{J}$ (or $\mathbf{B}$). The time dependence of these individual population ($G_j(t)$) and energy distribution ($\mathbf{g}_j(t)$) components is governed by the simple kinetic eqs 21 and 22. Changes in $G_j(t)$ and $\mathbf{g}_j(t)$ can be interpreted as due to (1) unimolecular reaction with rate constant $-\lambda_j$, (2) reactions with other species with pseudo-first-order rate constant $-u(t)$ (eq 7), and (3) formation via other reactions with effective flux $\theta_j(t)\Phi_j$ (or $\theta_j(t)\mathbf{e}_j$ for $\mathbf{g}_j(t)$) where $\theta_j(t)$ is given by eq 12. It is important that during the course of the reactions these individual components are in their individual steady states, i.e., time and energy dependencies are separated and changes occur only in the absolute values of $G_j(t)$ and $g_j(t)$ but not in the energy distribution shapes (determined by $\mathbf{e}_j$). The components evolve independently of each other, i.e., any change in $\mathbf{g}_{j1}(t)$ can influence $\mathbf{g}_{j2}(t)$ ($j1 \neq j2$) only indirectly via changes in concentrations of other species which, in turn, may result in changes to the time-dependent parameters $u(t)$ and $\theta_j(t)$. For practical purposes, it is convenient to treat the overall population of species A as consisting of these virtual steady-state "components" A_j, each with its population distribution function $\mathbf{g}_j(t)$. Then, $[A] = \sum_j [A_j]$ and $[A_j] \equiv G_j(t)$.

II.1.2. Effective Rate Constants of Reactions Involving Virtual A_j Components. Unimolecular Decay. The unimolecular decay of molecule A may result in several channels described as different reactions within the subset M2 (see eq 2) and indexed by m2. The formation rate of the products of reaction m2 caused by the unimolecular decay of $G(t)$ will be given by a sum of rates due to individual j-th components.

$$w^{m2}(t) = \left(\frac{\partial[\text{products(m2)}]}{\partial t}\right)_{\text{from reac.m2}} = \sum_i k^{m2}(E_i)g(E_i,t)\delta E = \sum_j w_j^{m2}(t) \quad (23)$$

where

$$w_j^{m2}(t) = \sum_i k^{m2}(E_i)g_j(E_i,t)\delta E = \bar{k}_j^{m2}G_j(t) \quad (24)$$

Here, $\bar{k}_j^{m2}$, obtained by averaging $k^{m2}(E)$ over the shape of the j-th component distribution function

$$\bar{k}_j^{m2} = (\sum_i k^{m2}(E_i)e_j(E_i)\delta E)/\Phi_j \quad (25)$$

can be identified with the effective rate constant of unimolecular decay of A_j via reaction channel m2.

One can show that for each A_j, the sum of effective rate constants over all m2 channels must be equal to $-\lambda_j$.

$$\sum_{m2} \bar{k}_j^{m2} = -\lambda_j \quad (26)$$

For the time evolution of the overall population, we can write

$$\frac{dG(t)}{dt} = -\sum_i k(E_i)g(E_i)\delta E + u(t)G(t) + \sum_i r(E_i,t)\delta E$$

At the same time, from eqs 17 and 22 we have

$$\frac{dG(t)}{dt} = \sum_j \lambda_j G_j(t) + u(t)G(t) + \sum_i r(E_i,t)\delta E$$

Thus, $-\sum_j \lambda_j G_j(t) = \sum_i k(E_i)g(E_i)\delta E = \sum_j \sum_i k(E_i)g_j(E_i)\delta E$. Equating terms with the same time dependencies, we obtain for each j $\lambda_j = -(\Phi_j)^{-1}\sum_i k(E_i)e_j(E_i)\delta E = -\sum_{m2}\bar{k}_j^{m2}$ which coincides with eq 26.

Formation. The energy-dependent rate of formation of species A in reaction subset M1 (eq 2) can also be presented as a sum of contributions due to A_j:

$$\left(\frac{\partial \mathbf{g}(t)}{\partial t}\right)_{\text{from M1}} = \sum_j \left(\frac{\partial \mathbf{g}_j(t)}{\partial t}\right)_{\text{from M1}} \quad \text{and}$$

$$\left(\frac{\partial G(t)}{\partial t}\right)_{\text{from M1}} = \sum_j \left(\frac{\partial G_j(t)}{\partial t}\right)_{\text{from M1}}$$

which, in turn, can be expressed via rates of individual reactions from subset M1 (see eqs 8 and 12):

$$\left(\frac{\partial \mathbf{g}_j(t)}{\partial t}\right)_{\text{from M1}} = \theta_j(t)\mathbf{e}_j = (\mathbf{Sr},\mathbf{Se}_j)\mathbf{e}_j = \mathbf{e}_j\sum_i \frac{r(E_i,t)e_j(E_i)}{f(E_i)}\delta E =$$

$$\mathbf{e}_j\sum_i\sum_{m1}\frac{e_j(E_i)}{f(E_i)}k^{m1}x^{m1}(E_i)\delta E[\text{reactants(m1)}] =$$

$$\mathbf{e}_j(\Phi_j)^{-1}\sum_{m1}\tilde{k}_j^{m1}[\text{reactants(m1)}] \quad (27)$$

where

$$\tilde{k}_j^{m1} = k^{m1}\Phi_j\sum_i \frac{e_j(E_i)}{f(E_i)}x^{m1}(E_i)\delta E \quad (28)$$

Thus, the expression for the flux (rate of formation) of A_j virtual components of A from reactions of the M1 subset acquires the form

$$\left(\frac{\partial G_j(t)}{\partial t}\right)_{\text{from M1}} = \sum_{m1}\tilde{k}_j^{m1}[\text{reactants(m1)}] \quad (29)$$

where $\tilde{k}_j^{m1}$ is an effective rate constant of the formation of A_j in reaction m1. The sum of $\tilde{k}_j^{m1}$ over all j must be equal to the rate constant k^{m1} corresponding to the total flux of $G(t)$ from reaction m1. This, indeed, can be confirmed:

$$\sum_j \tilde{k}_j^{m1} = \sum_j k^{m1}\Phi_j(\mathbf{Se}_j,\mathbf{Sx}^{m1}) = k^{m1}\sum_j \Phi_j(\mathbf{c}_j,\mathbf{Sx}^{m1}) =$$

$$k^{m1}\sum_i\sum_j S_{ii}^{-1}c_j(E_i)(\mathbf{c}_j,\mathbf{Sx}^{m1})\delta E = k^{m1}\sum_i S_{ii}^{-1}S_{ii}x^{m1}(E_i)\delta E =$$

$$k^{m1}\sum_i x^{m1}(E_i)\delta E = k^{m1}$$

(we used here the representation of $\mathbf{Sx}^{m1}$ in terms of eigenvectors $\mathbf{c}_j$ of $\mathbf{B}$: $\mathbf{Sx}^{m1} = \sum_j \mathbf{c}_j(\mathbf{c}_j,\mathbf{Sx}^{m1})$).

II.1.3. Expansion of the Kinetic Scheme. The mutual independence of the $G_j(t) = [A_j]$ components of the overall population $G(t) = [A]$ and eqs 22, 24, and 29 which describe the temporal evolution of $G_j(t)$ allow us to expand eqs 2 governing the kinetics of species A in terms of virtual A_j constituents. This expansion of the kinetic scheme proceeds via the following algorithm.

(1) Each A-producing reaction m1 of the subset M1 is transformed into N (N is the total number of eigenvalues of matrix $\mathbf{B}$, $1 \le j \le N$) reactions indexed by the double index $\binom{m1}{j}$, each "producing" the component A_j. The rate constant of each "new" reaction $\binom{m1}{j}$ is $\tilde{k}_j^{m1}$ given by expression 28.

(2) Each reaction (or channel) m2 of the subset M2 is transformed into N unimolecular reactions $\binom{m2}{j}$ of A_j components, each "producing" Products(m2) with the first-order rate constant $\tilde{k}_j^{m2}$ given by expression 25.

(3) Each reaction m3 of A with other species (subset M3) is transformed into N analogous reactions $\binom{m3}{j}$ of A_j components producing Products(m3) with rate constants k^{m3}.

$$\begin{cases} \text{Reactants(m1)} \xrightarrow{\tilde{k}_j^{m1}} A_j & \binom{m1}{j},\ m1 \in M1 \\ \cdots\cdots \quad \cdots\cdots \quad \cdots\cdots & \\ A_j \xrightarrow{\tilde{k}_j^{m2}} \text{Products(m2)} & \binom{m2}{j},\ m2 \in M2 \\ \cdots\cdots \quad \cdots\cdots \quad \cdots\cdots & \\ A_j + \text{Reactants(m3)} \xrightarrow{k^{m3}} \text{Products(m3)} & \binom{m3}{j},\ m3 \in M3 \\ \cdots\cdots \quad \cdots\cdots \quad \cdots\cdots & \end{cases} \quad (30)$$

$(1 \le j \le N)$

(4) The initial "concentration" of component A_j is given by

$$[A_j(0)] = G_j(0) = \xi_j\Phi_j = \Phi_j\sum_i \frac{g_o(E_i)}{f(E_i)}e_j(E_i)\delta E \quad (31)$$

The resultant total kinetic scheme consisting of all reactions not included in (M1, M2, M3) and the virtual reactions of eq 30 can be solved by any method normally used in macroscopic kinetics. However, the total number of kinetic equations can become exceedingly large since the number of virtual reactions in eq 30 equals N multiplied by the number of original reactions in subsets M1, M2, and M3. Fortunately, this very large scheme can be significantly simplified, as shown in the next section.

II.2. Reduction of the Large Modified Kinetic Scheme. *II.2.1. Spectra of Eigenvalues and Shapes of Eigenvectors.* Let us arrange all eigenvalues in order of their increasing absolute values ($|\lambda_1| \le |\lambda_2| \le \ldots |\lambda_N|$). The smallest (in absolute value) eigenvalue of matrixes $\mathbf{J}$ and $\mathbf{B}$, λ_1, is identified with the steady-state rate constant of thermal unimolecular decomposition of species A (see, for example, ref 9). The eigenvector $\mathbf{e}_1$ gives the corresponding steady-state energy distribution. It has been shown (ref 13) that, for a matrix without $k(E)$ (see eq 5), other

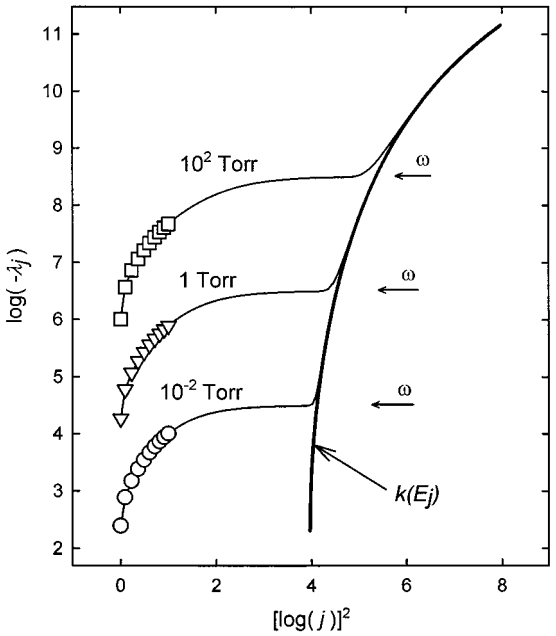

Figure 1. Spectrum of eigenvalues of the matrix **J** (and **B**) for the decomposition of *n*-C_4H_9 radicals at several pressures (T = 1500 K, O_2 as bath gas). To avoid plot congestion, only the first 10 eigenvalues at each pressure are represented with symbols and $|\lambda_j|$ vs j dependence is shown by lines for all other j: (○) pressure of 1.33 Pa (10^{-2} Torr); (▽) 133.3 Pa (1 Torr); (□) 1.33×10^4 Pa (100 Torr). Arrows show the corresponding values of the collisional frequency, ω. The heavy solid line represents the $k(E)$ vs E dependence.

eigenvalues correspond to the rates of collisional relaxation of A. For the full matrix, if $k(E)$ are not negligible compared with the collision rate (ω), they will influence the spectrum of eigenvalues. At sufficiently high energies, $k(E)$ become substantially higher than ω and the corresponding nondiagonal elements of matrix **J** (and **B**) become negligible compared with the diagonal ones which, in turn, are approximately equal to $-k(E)$ (see eq 5). This brings into the spectrum of eigenvalues $\lambda_j \approx -k(E_j)$ for such j that $k(E_j) \gg \omega$. The corresponding eigenvectors are localized in the vicinity of E_j (see, for example, ref 1).

Figure 1 demonstrates the spectrum of eigenvalues of a typical reactive system at several pressures. To avoid plot congestion, only the first 10 eigenvalues at each pressure are represented with symbols and $|\lambda_j|$ vs j dependence is shown by lines for all other j. One can see that the spectrum can be qualitatively divided into three parts: (1) several (5−10 in this case) eigenvalues which are significantly lower than the collision frequency ω, (2) eigenvalues approximately equal to the collision frequency ($|\lambda_j| \approx \omega$), and (3) eigenvalues approximately equal to microscopic rate constants ($|\lambda_j| \approx k(E_j)$). The corresponding shapes of the eigenvectors are illustrated in Figure 2.

While the shape of $e_1(E)$ represents the steady-state distribution of the thermal unimolecular reaction (see above and ref 9), other eigenvectors have very little physical meaning. As can be seen from Figure 2, these $e_j(E)$ dependencies may even change sign at some energies. Their integral characteristics (such as $G_j(t)$, $\bar{k}_j^{m1}$, and $\tilde{k}_j^{m1}$) can acquire negative values. This stresses the virtual nature of the A_j components introduced here for the ease of analysis.

II.2.2. Reduction of the Kinetic Scheme. In kinetic models of large systems (eq 1), generally, all bimolecular reactions have characteristic rates which are lower than the frequency of collisions with the bath gas ω. In pertinence to the kinetic

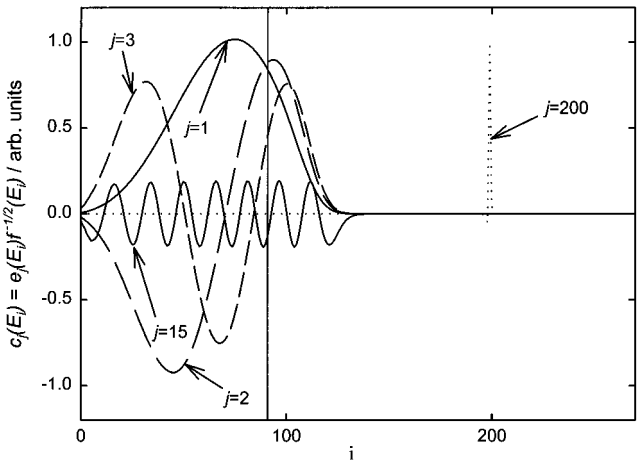

Figure 2. Shapes of eigenvectors $\mathbf{c}_j$ of the master equation matrix **B**. Decomposition of *n*-C_4H_9 radicals at 133.3 Pa (1 Torr) of O_2 and 1500 K.

scheme in eq 30, this means that for each virtual A_j component of the overall population of species A such that the corresponding eigenvalue $|\lambda_j|$ is approximately equal to or higher than ω, kinetics described by eq 30 will happen "instantly" on the time scale of the overall kinetics of the system. For these A_j, reactions of the subset M3 can be neglected since their rates are significantly slower than those of reactions ($_j^{m2}$) (m2 ∈ M2, overall rate constant $|\lambda_j|$).

Therefore, for each j with large enough $|\lambda_j|$, the scheme of eq 30 can be replaced by a set of "direct" multichannel reactions corresponding to the original reactions m1, different channels of which result in products of reactions m2.

$$\textit{Reactants(m1)} \rightarrow \begin{cases} \longrightarrow & \cdots\cdots\cdots\cdots \\ \xrightarrow{k_j^{m1,m2-1}} & \textit{Products(m2}-1\textit{)} \\ \xrightarrow{k_j^{m1,m2}} & \textit{Products(m2)} \\ \xrightarrow{k_j^{m1,m2+1}} & \textit{Products(m2}+1\textit{)} \\ \longrightarrow & \cdots\cdots\cdots\cdots \end{cases} \tag{32}$$

Here, individual channel rate constants are given by

$$k_j^{m1,m2} = \tilde{k}_j^{m1}\left(\frac{\bar{k}_j^{m2}}{\sum_{m2}\bar{k}_j^{m2}}\right) = \tilde{k}_j^{m1}\,\bar{k}_j^{m2}|\lambda_j|^{-1} \tag{33}$$

Furthermore, since we have the same sets of reactions M2 and M3 for all j, the scheme of eq 32 can be summed over all sufficiently large eigenvalues to result in only several multichannel reactions:

$$\textit{Reactants(m1)} \rightarrow \begin{cases} \longrightarrow & \cdots\cdots\cdots\cdots \\ \xrightarrow{k^{m1,m2-1}} & \textit{Products(m2}-1\textit{)} \\ \xrightarrow{k^{m1,m2}} & \textit{Products(m2)} \\ \xrightarrow{k^{m1,m2+1}} & \textit{Products(m2}+1\textit{)} \\ \longrightarrow & \cdots\cdots\cdots\cdots \end{cases} \tag{34}$$

where

$$k^{m1,m2} = \sum_{j\geq J} k_j^{m1,m2} = \sum_{j\geq J} \tilde{k}_j^{m1}\,\bar{k}_j^{m2}|\lambda_j|^{-1} \tag{35}$$

Here, we have chosen J such that all $|\lambda_j|$ are large enough for all $j \geq J$.

The initial "concentrations" of A_j given by eq 31 will be transformed into increments of concentrations of Products(m2) due to the "instant" reactions ($_j^{m2}$), i.e., the initial concentrations of Products(m2) need to be increased by

$$\Delta[\text{products(m2)}] = \sum_{j\geq J}\bar{k}_j^{m2}|\lambda_j|^{-1}G_j(0) = \sum_{j\geq J}|\lambda_j|^{-1}\left(\sum_i k^{m2}(E_i)e_j(E_i)\delta E\right)\left(\sum_i \frac{g_o(E_i)}{f(E_i)}e_j(E_i)\delta E\right) \quad (36)$$

The practical computation of $k^{m1,m2}$ and Δ[products(m2)] can be somewhat simplified by the use of a "correlation function" $b^{m2}(E)$,

$$b^{m2}(E) = \sum_{j\geq J}\Phi_j\gamma_j^{m2}e_j(E) \quad (37)$$

where

$$\gamma_j^{m2} = \frac{\sum_i k^{m2}(E_i)e_j(E_i)\delta E}{\sum_i k(E_i)e_j(E_i)\delta E} = \frac{\sum_i k^{m2}(E_i)e_j(E_i)\delta E}{\Phi_j|\lambda_j|} \quad (38)$$

has the meaning of an eigenvector-specific branching fraction for channel m*2*.

The physical meaning of the $b^{m2}(E)$ function can be understood from the fact that both $k^{m1,m2}$ and Δ[products(m2)] values are determined by the correlation, or overlap, between $b^{m2}(E)$, on the one side, and $x^{m1}(E)$ (the energy distribution of molecules formed in reaction m1) or $g_0(E)$ (the initial energy distribution), on the other (see eqs 25, 28, 35, and 36).

$$k^{m1,m2} = \sum_{j\geq J}\tilde{k}_j^{m1}\,\bar{k}_j^{m2}|\lambda_j|^{-1} = k^{m1}\sum_{j\geq J}\Phi_j\left(\sum_i \frac{e_j(E_i)}{f(E_i)}x^{m1}(E_i)\delta E\right)\times \frac{\sum_i k^{m2}(E_i)e_j(E_i)\delta E}{\sum_i k(E_i)e_j(E_i)\delta E} = k^{m1}\sum_{j\geq J}\Phi_j\gamma_j^{m2}\sum_i \frac{e_j(E_i)}{f(E_i)}x^{m1}(E_i)\delta E = k^{m1}\sum_i \frac{x^{m1}(E_i)}{f(E_i)}b^{m2}(E_i)\delta E \quad (39)$$

$$\Delta[\text{products(m2)}] = \sum_{j\geq J}|\lambda_j|^{-1}\left(\sum_i k^{m2}(E_i)e_j(E_i)\delta E\right)\times \left(\sum_i \frac{g_o(E_i)}{f(E_i)}e_j(E_i)\delta E\right) = \sum_i \frac{g_o(E_i)}{f(E_i)}b^{m2}(E_i)\delta E \quad (40)$$

II.3. Summary of Algorithm. (1) Analyze the reaction scheme of eq 2 by identifying each A-forming reaction of the subset M1 with a corresponding distribution function $\mathbf{x}^{m1}$ (energy distribution of A molecules formed in reaction m1) normalized such that $\sum_i x^{m1}(E_i)\delta E = 1$.

(2) For a particular temperature and pressure, find all N eigenvalues λ_j and corresponding eigenvectors $\mathbf{e}_j$ of the master equation matrix $\mathbf{J}$,

$$J_{i,l} = \begin{cases} R(E_i,E_l)\delta E, & i \neq l \\ -k(E_i) - \delta E\sum_{l\neq i}R(E_l,E_i), & i = l \end{cases} \quad (5)$$

(3) Select a "cutoff" factor F_{CO} such that all eigenvalue-specific unimolecular reactions ($_j^{m2}$) of virtual components A_j are considered as occurring "instantly" if the corresponding λ_j are such that

$$|\lambda_j| > \omega/F_{CO} \quad (41)$$

where ω is the collision frequency. The choice of the F_{CO} value is determined by the ratios of ω and the rates of the fastest bimolecular reactions of species A (in the unlikely case of these being comparable with ω, one can use $F_{CO} \leq 1$ or choose to solve the nonreduced modified kinetic scheme, which is more computationally demanding). Arrange all N eigenvalues such that λ_j satisfy the requirement of eq 41 for all $j \geq J$ and do not satisfy it for all $1 \leq j < J$. Here, J will be significantly less than the total number of eigenvalues N.

(4) The reaction scheme of eq 2 is transformed into J schemes. The first $J-1$ of these schemes (described by eq 30) involve virtual j-specific components A_j with rate constants given by expressions 25 and 28,

$$\bar{k}_j^{m2} = \left(\sum_i k^{m2}(E_i)e_j(E_i)\right)/\Phi_j \quad (25)$$

$$\tilde{k}_j^{m1} = k^{m1}\Phi_j\sum_i \frac{e_j(E_i)}{f(E_i)}x^{m1}(E_i) \quad (28)$$

where

$$\Phi_j = \sum_i e_j(E_i)\delta E \quad (18)$$

The last, J-th scheme is described by eq 34 and consists of "direct" multichannel reactions (not involving A or A_j) with rate constants for individual channels leading from (Reactants-(m1)) to (Products(m2)) given by

$$k^{m1,m2} = \sum_{j\geq J}k_j^{m1,m2} = \sum_{j\geq J}\tilde{k}_j^{m1}\,\bar{k}_j^{m2}|\lambda_j|^{-1} \quad (35)$$

where $\tilde{k}_j^{m1}$ and $\bar{k}_j^{m2}$ are computed via formulas 25 and 28. Initial "concentrations" of A_j are given by eq 31 and those of Products-(m2) by eq 36 (also see eqs 39 and 40).

Thus, the initial overall reaction scheme of eq 1 which involved non-steady-state kinetics of species A is reduced to a slightly larger kinetic scheme where all A-involving reactions are substituted with pseudoreactions described by eqs 30 and 34. The main benefit of this substitution is that the resultant overall reaction scheme involves only "normal" reactions with time-independent rate constants. This overall scheme can thus be solved using any ordinarily applied method.

III. Applications

III.1. Decomposition of *n*-C_4H_9 Radical. We consider the kinetics of decomposition of *n*-butyl radicals which are formed in two different processes: (1) hydrogen atom abstraction from *n*-C_4H_{10} and (2) thermal decomposition of *n*-butyl iodide, *n*-C_4H_9I. These two processes result in distinctly different initial energy distributions of the *n*-C_4H_9 formed. While the abstraction reaction is not likely to significantly deplete the energy of those vibrational modes of *n*-butane that will remain in the butyl

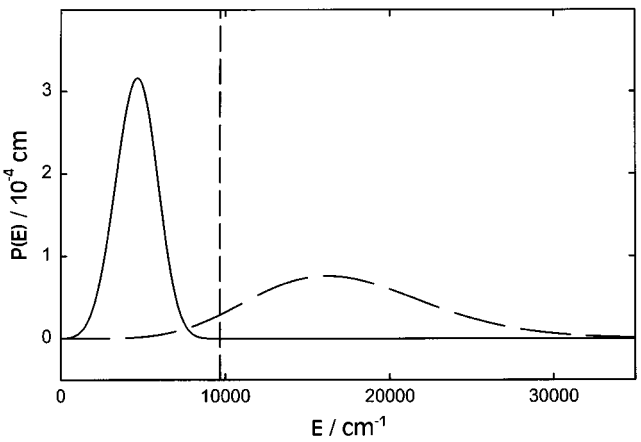

Figure 3. Energy distribution of n-C_4H_9 radicals produced in the unimolecular decomposition of n-C_4H_9I (solid line) and in abstraction reactions (dashed line, Boltzmann distribution) at 1500 K and 133.3 Pa (1 Torr) of O_2 (bath gas). Vertical line indicates the n-C_4H_9 decomposition reaction energy barrier.

fragment, the reaction of *n*-butyl iodide decomposition will leave the formed butyl radicals relatively cold.

To compute the energy distribution of *n*-butyl radicals formed in the decomposition of n-C_4H_9I, the formulas of the "prior distribution" method[14] were used. The fraction of n-C_4H_9 formed with vibrational energy E_1 from decomposition of n-C_4H_9I with total energy E is given by[14]

$$P(E_1|E)\,\mathrm{d}E_1 = \frac{\rho_1(E_1)\,\mathrm{d}E_1}{N(E)}\int_0^{E-E_1}\int_0^{E-E_1-E_t}\rho_t(E_t)\rho_r(E_r)\rho_2(E - E_t - E_r - E_1)\,\mathrm{d}E_r\,\mathrm{d}E_t$$

where the normalization integral

$$N(E) = \int_0^{E}\int_0^{E-E_1}\int_0^{E-E_1-E_t}\rho_t(E_t)\rho_r(E_r)\rho_1(E_1)\rho_2(E - E_t - E_r - E_1)\,\mathrm{d}E_1\,\mathrm{d}E_r\,\mathrm{d}E_t$$

$\rho_1(E_1)$ and $\rho_2(E_2)$ are densities of states of vibrational degrees of freedom of n-C_4H_9 and I atom (δ-function), and $\rho_t(E_t)$ and $\rho_r(E_r)$ are translational and rotational densities of states of products. As has been discussed by Baer and Hase (see ref 14, section 9.1.1), two translational degrees of freedom need to be included, which results in $\rho_t(E_t)$ being constant, $\rho_t(E_t) = R_t$. Since we are interested in energy distribution in all active degrees of freedom of n-C_4H_9 and not just vibrational ones, one active one-dimensional overall rotation is added to $\rho_1(E_1)$. Thus, $\rho_r(E_r)$ accounts for only two rotational degrees of freedom and, therefore, is constant: $\rho_r(E_r) = R_r$. Since $\rho_2(E_2) = \delta(E_2)$, we obtain for $P(E_1|E)$

$$P(E_1|E) = \frac{\rho_1(E_1)(E - E_1)}{\int_0^{E}\rho_1(E_1)(E - E_1)\,\mathrm{d}E_1}$$

To obtain the overall energy distribution in the active modes of n-C_4H_9 formed in the decomposition of n-C_4H_9I, one needs to average $P(E_1|E)$ over the energy-dependent flux of decomposing n-C_4H_9I molecules, $F(E) = k(E)g(E)$ where $k(E)$ and $g(E)$ are the energy-dependent microscopic rate constants and steady-state population distribution of n-C_4H_9I, respectively. Figure 3 illustrates the population energy distributions of n-C_4H_9 formed in the abstraction reaction (assumed to coincide with the Boltzmann distribution at 1500 K) and in the decomposition of *n*-butyl iodide.

The geometry and vibrational frequencies of n-C_4H_9I were obtained in ab initio calculations (GAUSSIAN 94,[15] UHF/6-31G* with LANL2DZ basis for iodine, results are listed in Appendix). The properties of the transition state for n-C_4H_9I decomposition (Appendix) were selected to reproduce the high-pressure limit Arrhenius dependence $k = 5 \times 10^{14}\exp(-52$ kcal mol$^{-1}/RT)$ s^{-1} (based on analogy with the decomposition of *n*-pentyl iodide[16]). The model of the n-C_4H_9 decomposition reaction was taken from Knyazev and Slagle.[17] Calculations were performed for the temperature of 1500 K and pressure of 133.3 Pa (1 Torr) (O_2 as bath gas). The exponential-down model[9,18] of collisional energy transfer was used. The selected value of the average energy transferred per collision was $\langle\Delta E\rangle_{all} = -30$ cm^{-1} (corresponding to $\langle\Delta E\rangle_{down} = 192$ cm^{-1} at 1500 K). The same value of $\langle\Delta E\rangle_{down}$ was used for n-C_4H_9I decomposition.

Solutions of the master equation (eigenvalues and eigenvectors of matrix **J**) were obtained via the method based on Householder's tridiagonalization algorithm[19] which was used earlier by Bedanov et al.[20] and Tsang et al.[5] Calculations were performed with an energy bin size $\delta E = 30$ cm^{-1} and matrix size 1400 × 1400. The kinetics of *n*-butyl radicals was analyzed using five virtual components corresponding to the first five eigenvalues of the corresponding master equation matrix **J**. The cutoff for eigenvalues (λ_j) was based on the requirement $\lambda_j < \omega/10$ ($F_{CO} = 10$; $\omega = 3.28 \times 10^6$ s^{-1} is the frequency of collisions with the bath gas). Rate constants for the formation of each of the virtual components were calculated via eq 28. Conversion factors between initial concentrations of n-C_4H_9 and those of virtual components were obtained via eq 31. Rate constants for the "direct" instantaneous reaction (accounting for contributions of all eigenvectors with high eigenvalues) were obtained via eq 39 and increments of product concentrations due to this "direct" reaction via eq 40. All calculated virtual component parameters for the two *n*-butyl radical energy distributions used are listed in Table 1.

Figure 4 illustrates the kinetics of n-C_4H_9 formed in the abstraction reaction, decomposition reaction, and in a combination of both abstraction and decomposition. Calculated concentration vs time profiles obtained from (1) the exact solution of a corresponding time-dependent master equation, (2) kinetic analysis based on the algorithm described above with five virtual components taken into account, and (3) the steady-state master equation solution are compared. As can be seen from the plots, at reaction times longer than $10/\omega$, good agreement between the current kinetic analysis based on the explicit treatment of virtual components and the exact master equation solution is achieved.

III.2. Oxidative Pyrolysis of an n-C_4H_9I/n-C_4H_{10} Mixture. We consider a simplified kinetic scheme of oxidative pyrolysis of a mixture of *n*-butyl iodide (0.1%), *n*-butane (5%), and oxygen (remaining 94.9%) at 1500 K and a pressure of 133.3 Pa (1 Torr). The elementary reactions involved are listed in Table 2. The process is initiated by reaction 1, the thermal decomposition of *n*-butyl iodide producing *n*-butyl radicals with relatively low energies (see section III.1). n-C_4H_9 radicals can either decompose to C_2H_5 and C_2H_4 (reaction 2) or react with O_2 forming 1-butene and HO_2 (reaction 4). Subsequent decomposition of ethyl radicals into ethylene and H atom results in appearance of OH and O atoms (via reaction H + O_2 → OH + O) which abstract hydrogen atoms from butane forming secondary and normal butyl radicals. These butyl radicals formed in

TABLE 1: Virtual Component Rate Constants for Decomposition of *n*-C_4H_9 and *sec*-C_4H_9 Radicals at 1500 K and 133.3 Pa (1 Torr) of O_2

j[a]	$\tilde{k}_j^{m1}/k^{m1}$	$\bar{k}_j^{m2}$ [b]	Φ_j	$[A_j(0)]/[A(0)]$	$k^{m1,m2}/k^{m1}$	Δ[products(m2)]/[A(0)]
			n-C_4H_9 Formed in Decomposition of *n*-C_4H_9I			
1	2.073	18616.5	−0.287	2.073		
2	−1.806	60716	0.153	−1.806		
3	0.981	1.187×10^5	−0.116	0.981		
4	−0.238	1.906×10^5	−0.100	−0.238		
5	−0.0524	2.743×10^5	0.0924	−0.0524		
					0.0425[c]	0.0425[c]
			n-C_4H_9 Formed in Abstraction Reactions (Boltzmann Distribution)			
1	0.0824	18616.5	−0.287	0.0824		
2	0.0233	60716	0.153	0.0233		
3	0.0135	1.187×10^5	−0.116	0.0135		
4	0.0101	1.906×10^5	−0.100	0.0101		
5	0.00854	2.743×10^5	0.0924	0.00854		
					0.8622[c]	0.8622[c]
			sec-C_4H_9 Formed in Abstraction Reactions (Boltzmann Distribution)			
1	0.1422	13210	0.3770	0.1422		
2	0.0331	47196	−0.1818	0.0331		
3	0.0171	94957	−0.1308	0.0171		
4	0.0116	1.553×10^5	−0.1075	0.0116		
5	0.00897	2.269×10^5	−0.0947	0.00897		
					0.7872[c]	0.7872[c]

[a] Virtual component number. [b] Coincides with the corresponding eigenvalue since only one reaction channel has nonnegligible rate. [c] Parameters for "direct" reaction.

abstraction reactions have Boltzmann energy distributions and decompose significantly faster than those formed in the decomposition of *n*-butyl iodide. Reactions involving two species display non-steady-state effects, those of formation and decomposition of *n*-C_4H_9 and *sec*-C_4H_9. The treatment of non-steady-state behavior in the *n*-butyl radical decomposition was described in section III.1. Decomposition of secondary butyl radical (reaction 12) was treated in a similar manner. The kinetics of five virtual components was considered explicitly. The model of reaction 12 was taken from Knyazev and Slagle.[25] Rate constants of the reactions producing virtual components of butyl radical were calculated via eq 28 and those of "direct" instantaneous reactions via eq 39. The resultant modified kinetic scheme and corresponding rate constants are presented in Table 3.

The modified kinetic scheme was solved using the CHEMKIN[26] program package. For comparison, the kinetic scheme of Table 2 (non-steady-state effects are ignored and the rate constants of butyl decomposition are obtained under a steady-state master equation approximation) was also solved for the same conditions. Figures 5−7 illustrate the kinetics of selected stable products and butyl radicals obtained (1) under the steady-state approximation and (2) using the method of accounting for non-steady-state kinetics described in the current work. As can be seen from the plots, the two different approaches result in significant differences in concentration vs time profiles. Figure 7 illustrates kinetics of individual virtual components of *n*-C_4H_9 as well as the overall [*n*-C_4H_9] vs time profile. As discussed in section II.2.2, virtual components have no physical meaning, and it is not surprising that concentrations of some of them acquire negative values.

IV. Discussion

The only two quantitative experimental studies of non-steady-state effects in reactions of polyatomic molecules are those of Kiefer et al.[3] and Fulle et al.[27] Kiefer et al. were able to quantitatively determine incubation times for the thermal dissociation of norbornene in shock tubes using the laser schlieren technique. These incubation times correspond to a time delay required for a transition from the room-temperature distribution of molecules to the higher energy steady-state

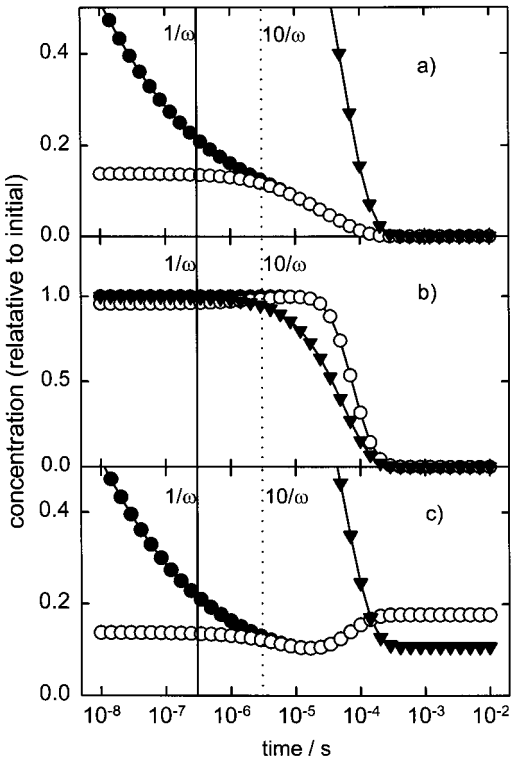

Figure 4. Concentration vs time profiles obtained in modeling of the *n*-C_4H_9 decomposition at 1500 K and 133.3 Pa (1 Torr) of O_2 via the exact solution of the time-dependent master equation (●), the current algorithm based on the explicit accounting for the first five virtual components (○), and the steady-state solution (▼): (a) Initial energy distribution of *n*-C_4H_9 is thermal (Boltzmann); (b) initial distribution is located mostly at low energies (from the thermal decomposition of *n*-C_4H_9I); (c) combination of initial Boltzmann distribution and a constant flux of *n*-C_4H_9 from the decomposition of *n*-C_4H_9I, 2000 molecules s^{-1}). Vertical lines mark reaction times equal to $1/\omega$ (solid line) and $10/\omega$ (dotted line) where ω is the frequency of collisions with the bath gas. The plot indicates a good convergence between the exact results and those obtained via the current method at all times longer than $10/\omega$.

TABLE 2: Reactions Included in the Simplified Mechanism of *n*-C_4H_9I/*n*-C_4H_{10}/O_2 Oxidative Pyrolysis

no.	reaction	rate constant[a]	ref
1	$C_4H_9I \rightarrow n\text{-}C_4H_9 + I$	2496.8[b]	
2	$n\text{-}C_4H_9 \rightarrow C_2H_5 + C_2H_4$	18616.5[c]	17
3	$C_2H_5 \rightarrow H + C_2H_4$	5192.0[d]	21
4	$n\text{-}C_4H_9 + O_2 \rightarrow 1\text{-}C_4H_8 + HO_2$	4.5×10^{-13}	22
5	$H + O_2 \rightarrow OH + O$	1.17×10^{-12}	23
6	$H + C_4H_{10} \rightarrow n\text{-}C_4H_9 + H_2$	8.45×10^{-12} [e]	24
7	$O + C_4H_{10} \rightarrow n\text{-}C_4H_9 + OH$	7.21×10^{-12} [e]	24
8	$OH + C_4H_{10} \rightarrow n\text{-}C_4H_9 + H_2O$	3.50×10^{-12} [e]	24
9	$O + C_4H_{10} \rightarrow sec\text{-}C_4H_9 + OH$	2.88×10^{-11} [e]	24
10	$OH + C_4H_{10} \rightarrow sec\text{-}C_4H_9 + H_2O$	6.97×10^{-12} [e]	24
11	$H + C_4H_{10} \rightarrow sec\text{-}C_4H_9 + H_2$	2.20×10^{-11} [e]	24
12	$sec\text{-}C_4H_9 \rightarrow CH_3 + C_3H_6$	13210[f]	25
13	$sec\text{-}C_4H_9 + O_2 \rightarrow 2\text{-}C_4H_8 + HO_2$	2.00×10^{-13}	22
14	$sec\text{-}C_4H_9 + O_2 \rightarrow 1\text{-}C_4H_8 + HO_2$	8.48×10^{-14}	22
15	$CH_3 + O_2 \rightarrow CH_2O + OH$	2.74×10^{-14}	23

[a] Rate constant units are s^{-1} and cm^3 $molecule^{-1}$ s^{-1}. [b] Calculated in the current work (see section III.1). [c] Calculated under steady-state assumption using the model of ref 17. [d] Calculated using the model of ref 21. [e] Calculated based on additivity coefficients of Warnatz.[24] [f] Calculated under steady-state assumption using the model of ref 25.

TABLE 3: Modified Mechanism of n-C_4H_9I/n-C_4H_{10}/O_2 Oxidative Pyrolysis

no.	reaction	rate constant[a]
1.1	$C_4H_9I \rightarrow NB1 + I$	5175.1
1.2	$C_4H_9I \rightarrow NB2 + I$	−4508.5
1.3	$C_4H_9I \rightarrow NB3 + I$	2448.5
1.4	$C_4H_9I \rightarrow NB4 + I$	−593.7
1.5	$C_4H_9I \rightarrow NB5 + I$	−130.9
1.6	$C_4H_9I \rightarrow C_2H_5 + C_2H_4 + I$	106.0
2.1	$NB1 \rightarrow C_2H_5 + C_2H_4$	18616.5
2.2	$NB2 \rightarrow C_2H_5 + C_2H_4$	60716
2.3	$NB3 \rightarrow C_2H_5 + C_2H_4$	1.187×10^5
2.4	$NB4 \rightarrow C_2H_5 + C_2H_4$	1.906×10^5
2.5	$NB5 \rightarrow C_2H_5 + C_2H_4$	2.743×10^5
3	$C_2H_5 \rightarrow H + C_2H_4$	5192.0
4.1	$NB1 + O_2 \rightarrow 1\text{-}C_4H_8 + HO_2$	4.5×10^{-13}
4.2	$NB2 + O_2 \rightarrow 1\text{-}C_4H_8 + HO_2$	4.5×10^{-13}
4.3	$NB3 + O_2 \rightarrow 1\text{-}C_4H_8 + HO_2$	4.5×10^{-13}
4.4	$NB4 + O_2 \rightarrow 1\text{-}C_4H_8 + HO_2$	4.5×10^{-13}
4.5	$NB5 + O_2 \rightarrow 1\text{-}C_4H_8 + HO_2$	4.5×10^{-13}
5	$H + O_2 \rightarrow OH + O$	1.17×10^{-12}
6.1	$H + C_4H_{10} \rightarrow NB1 + H_2$	6.963×10^{-13}
6.2	$H + C_4H_{10} \rightarrow NB2 + H_2$	1.971×10^{-13}
6.3	$H + C_4H_{10} \rightarrow NB3 + H_2$	1.140×10^{-13}
6.4	$H + C_4H_{10} \rightarrow NB4 + H_2$	8.519×10^{-14}
6.5	$H + C_4H_{10} \rightarrow NB5 + H_2$	7.217×10^{-14}
6.6	$H + C_4H_{10} \rightarrow C_2H_5 + C_2H_4 + H_2$	7.285×10^{-12}
7.1	$O + C_4H_{10} \rightarrow NB1 + OH$	5.941×10^{-13}
7.2	$O + C_4H_{10} \rightarrow NB2 + OH$	1.682×10^{-13}
7.3	$O + C_4H_{10} \rightarrow NB3 + OH$	9.724×10^{-14}
7.4	$O + C_4H_{10} \rightarrow NB4 + OH$	7.268×10^{-14}
7.5	$O + C_4H_{10} \rightarrow NB5 + OH$	6.158×10^{-14}
7.6	$O + C_4H_{10} \rightarrow C_2H_5 + C_2H_4 + OH$	6.216×10^{-12}
8.1	$OH + C_4H_{10} \rightarrow NB1 + H_2O$	2.880×10^{-13}
8.2	$OH + C_4H_{10} \rightarrow NB2 + H_2O$	8.153×10^{-14}
8.3	$OH + C_4H_{10} \rightarrow NB3 + H_2O$	4.714×10^{-14}
8.4	$OH + C_4H_{10} \rightarrow NB4 + H_2O$	3.523×10^{-14}
8.5	$OH + C_4H_{10} \rightarrow NB5 + H_2O$	2.985×10^{-14}
8.6	$OH + C_4H_{10} \rightarrow C_2H_5 + C_2H_4 + H_2O$	3.013×10^{-12}
9.1	$O + C_4H_{10} \rightarrow SB1 + OH$	4.093×10^{-12}
9.2	$O + C_4H_{10} \rightarrow SB2 + OH$	9.519×10^{-13}
9.3	$O + C_4H_{10} \rightarrow SB3 + OH$	4.924×10^{-13}
9.4	$O + C_4H_{10} \rightarrow SB4 + OH$	3.326×10^{-13}
9.5	$O + C_4H_{10} \rightarrow SB5 + OH$	2.582×10^{-13}
9.6	$O + C_4H_{10} \rightarrow CH_3 + C_3H_6 + OH$	2.266×10^{-11}
10.1	$OH + C_4H_{10} \rightarrow SB1 + H_2O$	9.905×10^{-13}
10.2	$OH + C_4H_{10} \rightarrow SB2 + H_2O$	2.304×10^{-13}
10.3	$OH + C_4H_{10} \rightarrow SB3 + H_2O$	1.192×10^{-13}
10.4	$OH + C_4H_{10} \rightarrow SB4 + H_2O$	8.051×10^{-14}
10.5	$OH + C_4H_{10} \rightarrow SB5 + H_2O$	6.248×10^{-14}
10.6	$OH + C_4H_{10} \rightarrow CH_3 + C_3H_6 + H_2O$	5.485×10^{-12}
11.1	$H + C_4H_{10} \rightarrow SB1 + H_2$	2.872×10^{-12}
11.2	$H + C_4H_{10} \rightarrow SB2 + H_2$	6.679×10^{-13}
11.3	$H + C_4H_{10} \rightarrow SB3 + H_2$	3.455×10^{-13}
11.4	$H + C_4H_{10} \rightarrow SB4 + H_2$	2.334×10^{-13}
11.5	$H + C_4H_{10} \rightarrow SB5 + H_2$	1.811×10^{-13}
11.6	$H + C_4H_{10} \rightarrow CH_3 + C_3H_6 + H_2$	1.590×10^{-11}
12.1	$SB1 \rightarrow CH_3 + C_3H_6$	13210
12.2	$SB2 \rightarrow CH_3 + C_3H_6$	47196
12.3	$SB3 \rightarrow CH_3 + C_3H_6$	94957
12.4	$SB4 \rightarrow CH_3 + C_3H_6$	1.553×10^5
12.5	$SB5 \rightarrow CH_3 + C_3H_6$	2.269×10^5
13.1	$SB1 + O_2 \rightarrow 2\text{-}C_4H_8 + HO_2$	2.00×10^{-13}
13.2	$SB2 + O_2 \rightarrow 2\text{-}C_4H_8 + HO_2$	2.00×10^{-13}
13.3	$SB3 + O_2 \rightarrow 2\text{-}C_4H_8 + HO_2$	2.00×10^{-13}
13.4	$SB4 + O_2 \rightarrow 2\text{-}C_4H_8 + HO_2$	2.00×10^{-13}
13.5	$SB5 + O_2 \rightarrow 2\text{-}C_4H_8 + HO_2$	2.00×10^{-13}
14.1	$SB1 + O_2 \rightarrow 1\text{-}C_4H_8 + HO_2$	8.48×10^{-14}
14.2	$SB2 + O_2 \rightarrow 1\text{-}C_4H_8 + HO_2$	8.48×10^{-14}
14.3	$SB3 + O_2 \rightarrow 1\text{-}C_4H_8 + HO_2$	8.48×10^{-14}
14.4	$SB4 + O_2 \rightarrow 1\text{-}C_4H_8 + HO_2$	8.48×10^{-14}
14.5	$SB5 + O_2 \rightarrow 1\text{-}C_4H_8 + HO_2$	8.48×10^{-14}
15	$CH_3 + O_2 \rightarrow CH_2O + OH$	2.74×10^{-14}

[a] Notations: NB1−NB5, virtual components of n-C_4H_9; SB1−SB5, virtual components of *sec*-C_4H_9. Rate constant units are s^{-1} and cm^3 $molecule^{-1}$ s^{-1}.

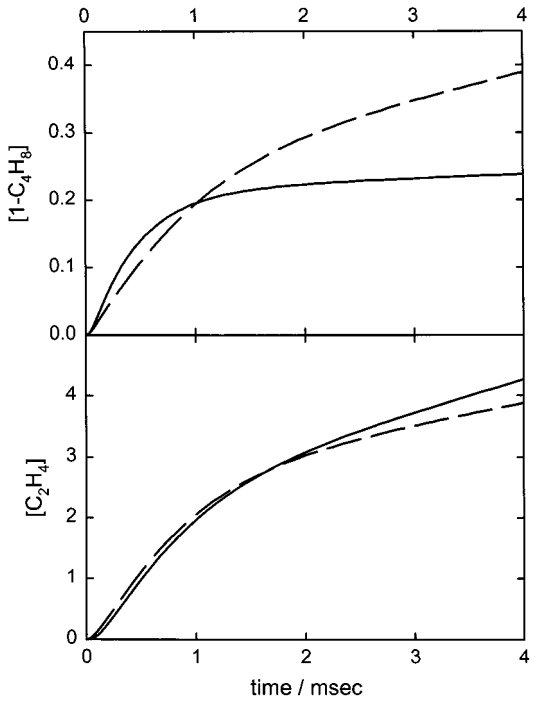

Figure 5. Concentration (mole fractions × 10^{-3}) vs time profiles of 1-butene and ethylene obtained in kinetic modeling of the oxidative pyrolysis of n-C_4H_9I/n-C_4H_{10}/O_2 mixture: (solid lines) results of modeling based on the current method of accounting for non-steady-state effects; (dashed lines) steady state is assumed in all unimolecular reactions. 1-butene and C_2H_4 are produced mainly via the competing reactions 4 (n-C_4H_9+O_2) and 2 (n-C_4H_9 decomposition), respectively. Steady-state approximation overpredicts the rate of n-C_4H_9 decomposition at shorter times (most of n-C_4H_9 is formed in n-C_4H_9I decomposition) and underpredicts it at longer times (most of n-C_4H_9 is formed in abstraction reactions) which is reflected in the temporal product concentration profiles.

distribution appropriate for a molecule in the falloff at high temperature. The experimental results of Kiefer et al. were modeled by Barker and King[4] who reproduced the observed kinetics via a solution of the time-dependent master equation. Using the same experimental technique, Fulle et al. estimated incubation times in the unimolecular decomposition of furane. In general, direct experimental information on non-steady-state effects is difficult to obtain because both of the competing processes (reaction and vibrational relaxation/activation) are very fast and, thus, not easily detectable in real-time experiments.

While experimental information is sparse, statistical unimolecular rate theory predicts the occurrence of non-steady-state effects in a large variety of reaction types (see Introduction). Such effects present a significant problem for the modeling of large kinetic schemes such as those found in combustion chemistry. Methods of solving complex kinetics are based on first establishing a mechanism (eq 1) characterized by time-independent rate coefficients. Then the corresponding system of linear differential equations is solved numerically to obtain concentration vs time profiles for all species involved (see, for example, ref 28). Non-steady-state effects result in kinetics which is not described by time-independent rate constants. If initial energy distributions and those of the activating processes are known, the resultant concentration vs time dependencies can be obtained via a solution of the corresponding master equation and fitted with phenomenological expressions to obtain time-dependent rate constants.[2,5] However, such an exercise, although illustrative, does not help to solve the overall complex kinetics since the temporal dependencies of the rate constants

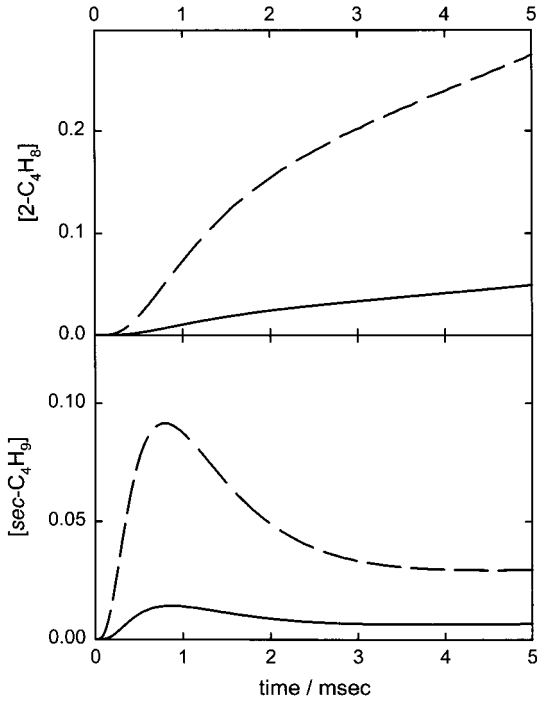

Figure 6. Concentration (mole fractions $\times 10^{-3}$) vs time profiles of 2-butene and secondary butyl radicals obtained in kinetic modeling of the oxidative pyrolysis of *n*-C_4H_9I/*n*-C_4H_{10}/O_2 mixture: (solid lines) results of modeling based on the current method of accounting for non-steady-state effects; (dashed lines) steady state is assumed in all unimolecular reactions.

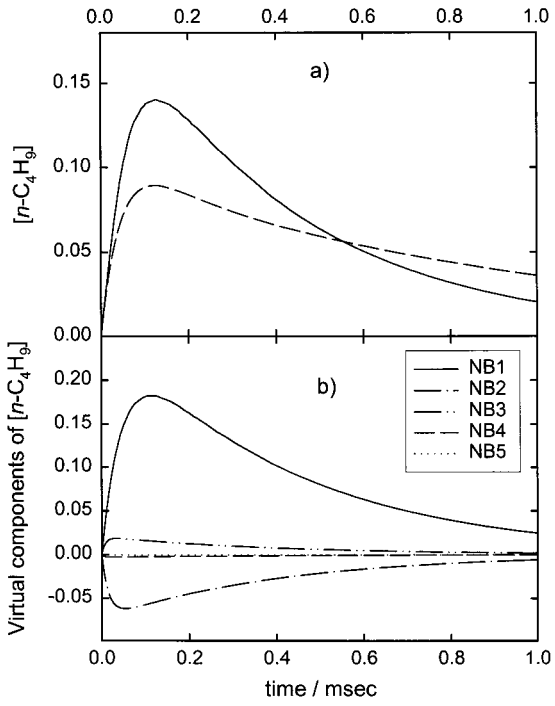

Figure 7. (a) Concentration (mole fractions $\times 10^{-3}$) vs time profile of *n*-C_4H_9 radicals obtained in kinetic modeling of the oxidative pyrolysis of *n*-C_4H_9I/*n*-C_4H_{10}/O_2 mixture: (solid line) results of modeling based on the current method of accounting for non-steady-state effects; (dashed line) steady state is assumed in all unimolecular reactions. (b) Concentration (mole fractions $\times 10^{-3}$) vs time profiles of the first five virtual components (NB1−NB5) of [*n*-C_4H_9].

are typically affected by several activation processes (such as different reactions producing the same chemical species), the balance of which changes during the overall process.

The current work is the first description of a method of accounting for non-steady-state kinetics in modeling large kinetic schemes. At present, the method is limited to cases of isothermal kinetics at constant pressure, i.e., conditions when the master equation needs to be solved numerically only once to obtain the eigenvalues and eigenvectors of matrixes **J** and **B** (see section II). Another limitation of the method is the assumption of energy independence of the rate constants of reactions between the affected species (A) and other molecules in the system. This assumption is reflected in the energy-independence of the $u(t)$ function in eqs 3 and 4. Unfortunately, our knowledge of the effects of vibrational excitation on bimolecular reaction rates is not as extensive as in the case of unimolecular reactions.[29] Since non-steady-state effects appear under conditions where the affected unimolecular reactions are very fast, only equally fast bimolecular reactions can compete with these unimolecular processes. Such fast reactions usually have very small or no energy barriers and their rate constants are not likely to be dramatically affected by vibrational excitation. Therefore, the assumption of energy independence of the rate constants of bimolecular reactions of species A (reactions of subset M3 in eq 2) is not likely to result in significant errors.

Chemically activated reactions represent a subset of the general case of unimolecular reactions. Traditionally, reactions of chemical activation are understood as those involving unimolecular transformations of an adduct formed by a recombination of two molecules.[9,10,30] The reactions of *n*-butyl and *sec*-butyl radicals considered in section III represent a somewhat different type of reactions activated chemically. The active molecule is formed not via recombination but in an abstraction reaction. However, the activated molecule is still characterized by vibrational excitation at energies significantly above the dissociation barrier, resulting in a considerable fraction of active molecules dissociating "instantly". This quick dissociation can be described in a way in which similar instantaneous channels of chemically activated reactions are frequently described, i.e., as a direct reaction bypassing the formation of the active molecule:

$$n\text{-}C_4H_{10} + OH \rightarrow C_2H_5 + C_2H_4 + H_2O$$

The general method described in section II for reactions affected by non-steady-state effects also provides treatment for systems (a specific case) where relaxation to the steady-state population energy distribution occurs quickly. In such instances, the kinetics of only one "virtual component" needs to be considered explicitly. If active molecules are created with high initial energies (chemical or photochemical activation), the "direct" reaction also needs to be included in the overall kinetic scheme. These systems with fast relaxation to a steady-state distribution correspond to the cases of steady-state thermal or chemically activated reactions extensively discussed in the literature (see, for example, refs 9 and 30 and references therein). For steady-state chemically activated reactions, the current method provides a formalism very similar to that of Smith et al.[8]

Acknowledgment. This research was supported by the National Science Foundation, Combustion and Thermal Plasmas Program under Grant CTS-9729287.

Appendix

Tables 4 and 5 contain structure and vibrational frequencies of *n*-C_4H_9I obtained in ab initio calculations and fitted transition state properties for the reaction of decomposition of *n*-C_4H_9I.

TABLE 4: Interatomic Distances, Angles, and Vibrational Frequencies of *n*-C_4H_9I Obtained in ab Initio Calculations (Symmetrical Structure with C1, C2, C3, C4, and I in the Plane of Symmetry)

parameter[a]	value	parameter[a]	value
IC1	2.1943	C3C2	1.5335
H32C3C2C4	121.8195	H21C2	1.085
H21C2C1C3	−121.3938	C4C3	1.5286
H11C1C2I	117.5994	H32C3	1.0874
H41C4	1.0851	H11C1C2	112.6965
H42C4	1.0859	C3C2C1	110.9503
H42C4C3	111.1497	H21C2C1	109.6912
H41C4C3	111.0205	C4C3C2	112.3834
H42C3C2H41	119.9791	H32C3C2	109.4712
C2C1	1.5191	C2C1I	112.4602
H11C1	1.0779	C3C2C1I	180.000

Rotational Constants (cm^{-1}): $B = 0.023591$ (two-dimensional), $B = 0.51106$ (one-dimensional)

Vibrational Frequencies (cm^{-1}):[b] 91.3,[c] 109.2,[c] 122.5, 228.4, 234.4,[c] 364.0, 552.6, 697.9, 739.6, 860.5, 876.0, 972.1, 1005.4, 1022.7, 1077.1, 1189.8, 1194.9, 1270.3, 1296.1, 1296.7, 1370.8, 1394.3, 1445.1, 1456.1, 1461.1, 1463.0, 1473.0, 2843.1, 2850.0, 2866.3, 2870.2, 2901.1, 2909.2, 2912.4, 2940.8, 3003.3

[a] Interatomic distances and angles in Å and degrees. [b] Scaled by a factor of 0.89. [c] These torsional frequencies were represented in modeling by hindered one-dimensional rotors with the following parameters (rotational constants, torsional barriers, symmetry numbers): (1) $B = 0.866$ cm^{-1}, $V = 1063$ cm^{-1}, $\sigma = 1$; (2) $B = 1.443$ cm^{-1}, $V = 915$ cm^{-1}, $\sigma = 1$; (3) $B = 5.748$ cm^{-1}, $V = 1062$ cm^{-1}, $\sigma = 3$.

TABLE 5: Model of the Transition State for the Reaction of Unimolecular Decomposition of *n*-C_4H_9I

Vibrational Frequencies (cm^{-1}): 110.0, 120.0, 190.0, 200.0, 400.0, 700.0, 876.0, 972.1, 1005.4, 1022.7, 1077.1, 1189.8, 1194.9, 1270.3, 1296.1, 1296.7, 1370.8, 1394.3, 1445.1, 1456.1, 1461.1, 1463.0, 1473.0, 2843.1, 2850.0, 2866.3, 2870.2, 2901.1, 2909.2, 2912.4, 2940.8, 3003.3

Rotational Constants (B), Torsional Barriers (V), and Symmetry Numbers (σ)

Overall Rotations	
2-dimensional	$B = 0.023591$ cm^{-1}; $\sigma = 1$
1-dimensional	$B = 0.51106$ cm^{-1}; $\sigma = 1$
Internal Rotations	
CH_3 torsion	$B = 5.74788$ cm^{-1}; $V = 1062$ cm^{-1}; $\sigma = 3$
C_2H_5 torsion	$B = 1.44278$ cm^{-1}; $V = 915$ cm^{-1}; $\sigma = 1$
C_3H_7 torsion	$B = 0.86564$ cm^{-1}; $V = 1063$ cm^{-1}; $\sigma = 1$

Reaction barrier height $E_0 = 211.15$ kJ mol^{-1}

References and Notes

(1) Schranz, H. W.; Nordholm, S. *Chem. Phys.* **1984**, *87*, 163.

(2) Bernshtein, V.; Oref, I. *J. Phys. Chem.* **1993**, *97*, 6830.

(3) Kiefer, J. H.; Kumaran, S. S.; Sundaram, S. *J. Chem. Phys.* **1993**, *99*, 3531.

(4) Barker, J. R.; King, K. D. *J. Chem. Phys.* **1995**, *103*, 4953.

(5) Tsang, W.; Bedanov, V.; Zachariah, M. R. *J. Phys. Chem.* **1996**, *100*, 4011.

(6) Kiefer, J. H. *Symp. (Int.) Combust., Proc.* **1998**, *27*, 113.

(7) Knyazev, V. D.; Slagle, I. R. *J. Phys. Chem. A* **1998**, *102*, 1770.

(8) Smith, S. C.; McEwan, M. J.; Gilbert, R. G. *J. Chem. Phys.* **1989**, *90*, 4265.

(9) Gilbert, R. G.; Smith, S. C. *Theory of Unimolecular and Recombination Reactions*; Blackwell: Oxford, 1990.

(10) Rabinovitch, B. S.; Diesen, R. W. *J. Chem. Phys.* **1959**, *30*, 735.

(11) Arfken, G. B.; Weber, H. J. *Mathematical Methods for Physicists*, 4th ed.; Academic Press: San Diego, 1995.

(12) Zwillinger, D. *Handbook of Differential Equations*; Academic Press: San Diego, 1998.

(13) Pritchard, H. O. *Quantum Theory of Unimolecular Reactions*; Cambridge University Press: Cambridge, 1984.

(14) Baer, T.; Hase, W. L. *Unimolecular Reaction Dynamics*; Oxford University Press: New York, 1996.

(15) Frisch, M. J.; Trucks, G. W.; Schlegel, H. B.; Gill, P. M. W.; Johnson, B. G.; Robb, M. A.; Cheeseman, J. R.; Keith, T.; Petersson, G. A.; Montgomery, J. A.; Raghavachari, K.; Al-Laham, M. A.; Zakrzewski, V. G.; Ortiz, J. V.; Foresman, J. B.; Cioslowski, J.; Stefanov, B. B.; Nanayakkara, A.; Challacombe, M.; Peng, C. Y.; Ayala, P. Y.; Chen, W.; Wong, M. W.; Andres, J. L.; Replogle, E. S.; Gomperts, R.; Martin, R. L.; Fox, D. J.; Binkley, J. S.; Defrees, D. J.; Baker, J.; Stewart, J. P.; Head-Gordon, M.; Gonzalez, C.; Pople, J. A. *Gaussian 94*, revision E.1; Gaussian, Inc.: Pittsburgh, PA, 1995.

(16) Tsang, W.; Walker, J. A.; Manion, J. A. *Symp. (Int.) Combust., Proc.* **1998**, *27*, 135.

(17) Knyazev, V. D.; Slagle, I. R. *J. Phys. Chem.* **1996**, *100*, 5318.

(18) Rabinovitch, B. S.; Tardy, D. C. *J. Chem. Phys.* **1966**, *45*, 3720.

(19) Wilkinson, J. H.; Reinsch, C. *Linear Algebra*; Springer: New York, 1971.

(20) Bedanov, V. M.; Tsang, W.; Zachariah, M. R. *J. Phys. Chem.* **1995**, *99*, 11452.

(21) (a) Knyazev, V. D. *J. Phys. Chem.* **1995**, *99*, 14738. (b) Feng, Y.; Niiranen, J. T.; Bencsura, A.; Knyazev, V. D.; Gutman, D. *J. Phys. Chem.* **1993**, *97*, 871.

(22) Baker, R. R.; Baldwin, R. R.; Fuller, A. R.; Walker, R. W. *J. Chem. Soc., Faraday Trans. 1* **1975**, *71*, 736.

(23) Baulch, D. L.; Cobos, C. J.; Cox, R. A.; Esser, C.; Frank, P.; Just, Th.; Kerr, J. A.; Pilling, M. J.; Troe, J.; Walker, R. W.; Warnatz, J. *J. Phys. Chem. Ref. Data* **1992**, *21*, 411.

(24) Warnatz, J. In *Combustion Chemistry*; Gardiner, W. C., Jr., Ed.; Springer-Verlag: New York, 1984.

(25) Knyazev, V. D.; Dubinsky, I. A.; Slagle, I. R.; Gutman, D. *J. Phys. Chem.* **1994**, *98*, 11099.

(26) Kee, R. J.; Rupley, F. M.; Miller, J. A. *CHEMKIN-2*, a FORTRAN chemical kinetics package for the analysis of gas-phase chemical kinetics; Code Package SAND89-8009, Sandia National Laboratories, 1989.

(27) Fulle, D.; Dib, A.; Kiefer, J. H.; Zhang, Q.; Yao, J.; Kern, R. D. *J. Phys. Chem. A* **1998**, *102*, 7480.

(28) Gardiner, W. C., Jr. In *Combustion Chemistry*; Gardiner, W. C., Jr., Ed.; Springer-Verlag: New York, 1984.

(29) Crim, F. F. *J. Phys. Chem.* **1996**, *100*, 12725.

(30) Robinson, P. J.; Holbrook, K. A. *Unimolecular Reactions*; Wiley-Interscience: New York, 1972.